

# Studies on cerium ( $\text{Ce}^{4+}/\text{Ce}^{3+}$ )–vanadium( $\text{V}^{2+}/\text{V}^{3+}$ ) redox flow cell—cyclic voltammogram response of $\text{Ce}^{4+}/\text{Ce}^{3+}$ redox couple in $\text{H}_2\text{SO}_4$ solution

Y. Liu<sup>a,\*</sup>, X. Xia<sup>b</sup>, H. Liu<sup>b</sup>

<sup>a</sup> Department of Chemistry, University of South Florida, Tampa, FL 33620, USA

<sup>b</sup> Institute of Applied Chemistry, Xinjiang University, Urumqi 830046, China

Received 13 November 2003; accepted 10 December 2003

## Abstract

A novel  $\text{Ce}^{4+}/\text{Ce}^{3+}-\text{V}^{2+}/\text{V}^{3+}$  redox flow cell has been designed. The electrochemical responses of higher concentration  $\text{Ce}^{4+}/\text{Ce}^{3+}$  couple in  $\text{H}_2\text{SO}_4$  solution were investigated via cyclic voltammetry. The normal potential and the kinetic parameters for anodic oxidation of  $\text{Ce}^{3+}$  and cathodic reduction of  $\text{Ce}^{4+}$  were measured. The results showed the surface of platinum electrode was fully covered with type I oxide that inhibited the reduction of  $\text{Ce}^{4+}$ . The reversibility of the  $\text{Ce}^{4+}/\text{Ce}^{3+}$  couple improved with the increase of  $\text{H}_2\text{SO}_4$  concentration. Different electrochemically active substances existed at various state of charge (SOC) and the reversibility of the  $\text{Ce}^{4+}/\text{Ce}^{3+}$  couple at the carbon electrode was superior to platinum.

© 2003 Published by Elsevier B.V.

**Keywords:** Redox flow cell; Cyclic voltammogram;  $\text{Ce}^{4+}/\text{Ce}^{3+}$  couple

## 1. Introduction

The  $\text{Ce}^{4+}/\text{Ce}^{3+}$  couple was chosen as the positive electrolyte of cerium ( $\text{Ce}^{4+}/\text{Ce}^{3+}$ )–vanadium ( $\text{V}^{2+}/\text{V}^{3+}$ ) redox flow cell [1,2] mainly for the high potential of  $\text{Ce}^{4+}/\text{Ce}^{3+}$  couple. If it was matched with a possible negative electrolyte, such as  $\text{V}^{2+}/\text{V}^{3+}$ , the theoretical open circuit voltage would be 1.96, 1.87, 1.7, 1.54 V (versus SHE) in  $\text{HClO}_4$ ,  $\text{HNO}_3$ ,  $\text{H}_2\text{SO}_4$  and  $\text{HCl}$  solutions, respectively, thoroughly satisfying the requirements of practical batteries. Also its open circuit voltage is higher than the conventional redox flow cells, such as Fe–Cr [3] (1.18 V versus SHE), Fe–Ti [4] (0.67 V versus SHE) and all vanadium [5] (1.26 V versus SHE) redox flow cells. Because of its high potential,  $\text{Ce}^{4+}$  was often used in the oxidative titration of  $\text{Fe}^{2+}$  [6],  $\text{I}^-$  [7], the oxidation of the organic molecular in waste water [8], the oxidation of  $\text{Cl}^-$  to  $\text{Cl}_2$  in chloralkali industry [9] and the oxidation of  $\text{H}_2\text{O}$  to  $\text{O}_2$  [10]. The reduction of  $\text{Ce}^{4+}$  at Pt, Au, Ir [11,12] highly boron-doped conductive diamond electrodes [12,13] and the oxidation of  $\text{Ce}^{3+}$  on Au, GC [14,15],  $\text{PbO}_2$  [16,17],  $\text{SnO}_2$  [8] electrodes were

investigated. Klekens et al. [18] reported that the reduction of  $\text{Ce}^{4+}$  was independent of the electrode materials; the charge-transfer coefficient ( $\alpha$ ) and the heterogeneous rate constant ( $k_c$ ) were similar for different electrodes, for instance, at Pt, Au, GC electrodes the  $k_c$  was  $3.7 \times 10^{-4} \text{ cm s}^{-1}$  [19],  $4.8 \times 10^{-4} \text{ cm s}^{-1}$  [20],  $3.8 \times 10^{-4} \text{ cm s}^{-1}$  [19], and  $\alpha$  was 0.21 [19], 0.35 [20], 0.28 [19], respectively. But as to the oxidation of  $\text{Ce}^{3+}$ , the various electrodes had different effects on the reaction of  $\text{Ce}^{3+} \rightarrow \text{Ce}^{4+} + \text{e}^-$ .

Here  $\text{H}_2\text{SO}_4$  was chosen as the acid media mainly because:

- (1) In  $\text{HClO}_4$  or  $\text{HNO}_3$  solution, the potential of  $\text{Ce}^{4+}/\text{Ce}^{3+}$  couple is high, and far above the overpotential for oxygen evolution, and the  $\text{Ce}^{4+}/\text{Ce}^{3+}$  couple is not stable in  $\text{HClO}_4$  or  $\text{HNO}_3$  solution [21,22]. Although the potential of the  $\text{Ce}^{4+}/\text{Ce}^{3+}$  couple is also high in  $\text{H}_2\text{SO}_4$  solution, Kunz [23] proved that  $\text{Ce}(\text{SO}_4)_2$  could stably exist in  $\text{H}_2\text{SO}_4$  solution, redox reaction seldom took place and the stability of the electrochemical active material is especially important in a redox flow cell.
- (2)  $\text{ClO}_4^-$  and  $\text{NO}_3^-$  cannot form stable complexes with  $\text{Ce}^{4+}$  and  $\text{Ce}^{3+}$  (this is also the reason that the potential of this couple is higher than that in  $\text{H}_2\text{SO}_4$  solution),

\* Corresponding author. Tel.: +1-813-335-7178; fax: +1-813-974-1733.  
E-mail address: [yliu17@helios.acomp.usf.edu](mailto:yliu17@helios.acomp.usf.edu) (Y. Liu).

### Nomenclature

$A$	the surface area of the working electrode
$c_j^*$	the bulk concentration of species $j$
$D_j$	the diffusion coefficient of species $j$
$E_p$	the peak potential
$E_{pa}$ and $E_{pc}$	the anodic and cathodic peak potential
$\Delta E_p$	the difference between cathodic and anodic peak potential
$I_p$	the peak current
$m$	the total numbers of scanning
$n$	the number of electrons involved in the rate-determining step
SOC	the state of charge
<i>Greek letters</i>	
$\alpha, \beta$	the cathodic and anodic transfer coefficient
$\nu$	the potential scan rate

however,  $\text{SO}_4^{2-}$  can form a complex with  $\text{Ce}^{4+}$ , in the form of  $\text{CeSO}_4^{2+}$ ,  $\text{Ce}(\text{SO}_4)_2$  and  $\text{Ce}(\text{SO}_4)_3^{2-}$  [13]. Because of the formation of a stable complex, it was generally accepted that the  $\text{Ce}^{4+}$  and  $\text{Ce}^{3+}$  would not undergo hydrolysis in  $\text{H}_2\text{SO}_4$  solution.

- (3) If trying to take HCl as the acid media, then  $\text{Ce}^{4+}$  would oxidize  $\text{Cl}^-$  to  $\text{Cl}_2$ . Mills [9] used the Ru, Ir oxide as the catalyst to accelerate this reaction, which demonstrated that the  $\text{Ce}^{4+}/\text{Ce}^{3+}$  couple was unstable in HCl solution.

Previous work was chiefly focused on electroanalysis, and the concentration of the  $\text{Ce}^{4+}/\text{Ce}^{3+}$  couple used was quite low,  $\text{mmol dm}^{-3}$ , but since the electroactive materials are used in redox flow cell, the concentrate should be large, therefore in this paper the concentration of  $\text{Ce}^{4+}$  and  $\text{Ce}^{3+}$  were both above  $0.1 \text{ mol dm}^{-3}$ . From the cyclic voltammogram response of a  $\text{Ce}^{4+}/\text{Ce}^{3+}$  couple at an inert working electrode, we investigated the reversibility of the couple in  $\text{H}_2\text{SO}_4$  solution. In addition, the kinetic parameters of the  $\text{Ce}^{4+}/\text{Ce}^{3+}$  couple and the oxidation efficiency of  $\text{Ce}^{3+}$  at various electrodes have been obtained by rotating disk electrode (RDE) and rotating ring-disk electrode (RRDE) [24]. The optimum  $\text{Ce}(\text{SO}_4)_2$  concentration was obtained through linear polarization [25]. The initial reaction mechanism of the  $\text{Ce}^{4+}/\text{Ce}^{3+}$  system was also proposed by means of the electrical impedance spectroscopy (EIS) technique [25]. The  $\text{Ce}^{4+}/\text{Ce}^{3+}-\text{V}^{2+}/\text{V}^{3+}$  redox cell was set up and the coulombic efficiency remained around 90% and the discharge voltage stabilized between 1.5 and 1.2 V [1]. Therefore as a completely new power system, the  $\text{Ce}^{4+}/\text{Ce}^{3+}$  redox couple is an attractive system and can be used in a redox flow cell.

## 2. Experimental

### 2.1. Apparatus and experiment steps

The curves of current versus potential were recorded in a 3-compartment cell, with Pt ( $0.2 \text{ cm}^2$ ), GC ( $0.16 \text{ cm}^2$ ), and Gr ( $1.13 \text{ cm}^2$ ) as inert working electrodes, respectively, the auxiliary electrode was a platinum sheet. All potentials were expressed relative to the  $\text{Hg}/\text{Hg}_2\text{SO}_4$  electrode, which was connected with the electrochemical cell through a salt bridge full of  $\text{H}_2\text{SO}_4$  electrolytic solution. The electrolytic solutions used were 0.5, 1.25, and  $2 \text{ mol dm}^{-3}$   $\text{H}_2\text{SO}_4$ , the cerium salts (analytical grade), including  $\text{Ce}(\text{SO}_4)_2 \cdot 4\text{H}_2\text{O}$  and  $\text{Ce}_2(\text{SO}_4)_3$ , were used as received. The cyclic voltammogram was measured by the CHI660 electrochemical station (CH Corporation, USA).

To get reproducible experimental data, the Pt electrode was pretreated as follows: a 10 min ultrasonication (JY92-2D ultrasonic cell pulverizer) was followed by potential cycling for 20 min at  $50 \text{ mV s}^{-1}$  between 1.80 and  $-0.6 \text{ V}$ , then a potential program (Scheme 1 in [19]) was used to record polarization curves for producing a layer of constant platinum oxide thickness.

By the above pretreatment the type I platinum oxide would reach an apparently limiting covered thickness. The glassy carbon electrode was cycled between 1.3 and  $-1.0 \text{ V}$  (versus SCE) for 10 min at a scan rate of  $0.03 \text{ V s}^{-1}$  after which it was held successively at 0.5 and 0 V (versus SCE) for 5 min. According to the above treatment, a reproducible GC electrode surface could be obtained [18]. Solutions were de-aerated 15 min by bubbling with nitrogen before each measurement.

### 2.2. The mathematical treatment of results

The peak current and the peak potential have the relationship as follows [13]:

$$E_p = \text{constant} - \left( \frac{RT}{2\alpha nF} \right) \ln \nu, \quad T = 298 \text{ K} \quad (1)$$

$$I_p = 299(\alpha n)^{1/2} A C_j^* D_j^{1/2} \nu^{1/2} \quad (2)$$

where  $E_p$  is the peak potential,  $\alpha$  the transfer coefficient,  $n$  the number of electrons involved in the rate-determining step,  $\nu$  the potential scan rate,  $I_p$  the peak current,  $A$  the surface area of the working electrode,  $c_j^*$  the bulk concentration of species  $j$  and  $D_j$  the diffusion coefficient of species  $j$ . From Eq. (1), the values of  $\alpha$ ,  $\beta$  (the cathodic and anodic transfer coefficient) can be obtained by the plot of  $E_p$  versus  $\ln \nu$ . Using the value of  $\alpha$ ,  $\beta$  obtained, a proportional relation between  $I_p$  and  $\nu^{1/2}$  can be observed, and  $D_j$  can also be easily obtained.

The peak current may be expressed as [26]:

$$I_p = 0.227nFAC_j^*k^0 \exp \left[ - \left( \frac{\alpha nF}{RT} \right) (E_p - E^{0'}) \right] \quad (3)$$

A plot of  $\ln(i_p)$  versus  $(E_p - E^{0'})$ , determined by different scan rates, should thus have a slope proportional to  $\alpha$  and an intercept proportional to  $k^0$ . The formal potential of the electrode ( $E^{0'}$ ) was estimated from the results of cyclic voltammogram [27]:

$$E^{0'} = \sum \frac{E_{pa} + E_{pc}}{2m} \quad (4)$$

where  $E_{pa}$  and  $E_{pc}$  are the anodic and cathodic peak potential, and  $m$  the total numbers of scanning.

### 3. Results and discussion

#### 3.1. The effect of preoxidation at the surface of Pt electrode on the $Ce^{4+}/Ce^{3+}$ couple

Due to the high potential of  $Ce^{4+}/Ce^{3+}$  couple, the metal electrode even including the noble metal, such as Pt, Au, etc. could not avoid being oxidized. From Fig. 1, it is easy to observe that the cathodic and the anodic current peaks are located between 0.4 and 0.9 V. Another small reduction peak current between 0 and  $-0.2$  V is the result of platinum oxide reduction. To investigate the effect of this oxide on the  $Ce^{4+}/Ce^{3+}$  couple, the sweep width ranged from 0 to 1.4 V (Fig. 2) to  $-0.2$  to 1.4 V (Fig. 3). Fig. 2 showed clearly that the existence of platinum oxide inhibited the oxidation of  $Ce^{3+}$ , especially while the sweep rate was fast, the distinct anodic peak could not be observed, which was attributed to the oxygen-evolution reaction. Compared with Fig. 2, in the cyclic voltammogram scanning from  $-0.2$  to 1.4 V (Fig. 3), the surface oxide of platinum metal could be partly eliminated (under high potential conditions, there was no way to completely reduce the platinum oxide, even if it could be achieved, while scanning toward the anodic direction, the platinum oxide could be produced again). Due to the similarity of the oxygen-evolution current and potential to the two different scan widths, this difference cannot be attributed to the oxygen-evolution reaction which made the anodic current peak of  $Ce^{3+}$  disappear.

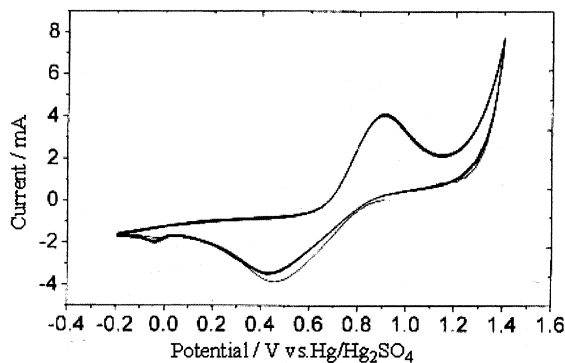


Fig. 1. Plot of cyclic voltammogram in  $0.3 \text{ mol dm}^{-3} \text{ Ce(SO}_4)_2 + 2 \text{ mol dm}^{-3} \text{ H}_2\text{SO}_4$  solution, sweep rate is  $0.05 \text{ V s}^{-1}$  at Pt electrode.

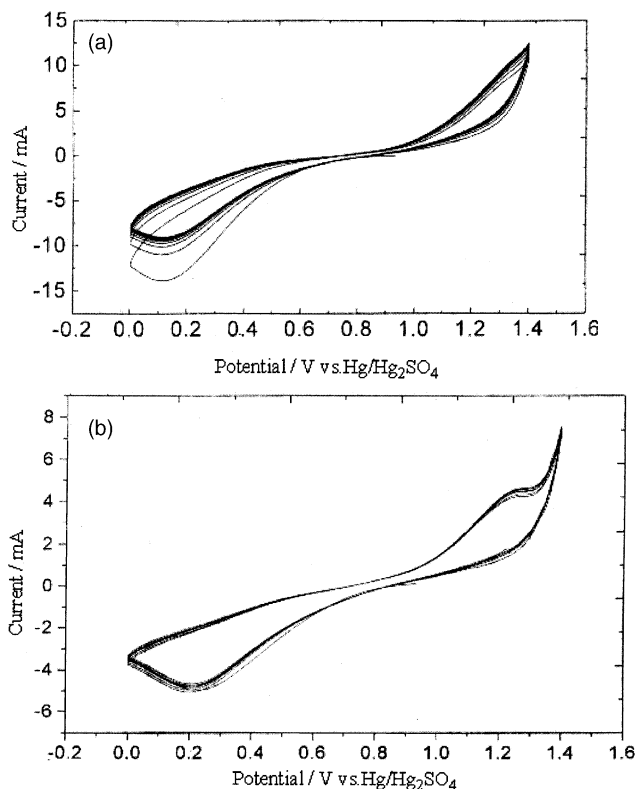


Fig. 2. Plot of cyclic voltammogram in  $0.3 \text{ mol dm}^{-3} \text{ Ce(SO}_4)_2 + 1.25 \text{ mol dm}^{-3} \text{ H}_2\text{SO}_4$  solution; sweep rate: (a)  $0.25 \text{ V s}^{-1}$  and (b)  $0.05 \text{ V s}^{-1}$  (between 0 and 1.4 V).

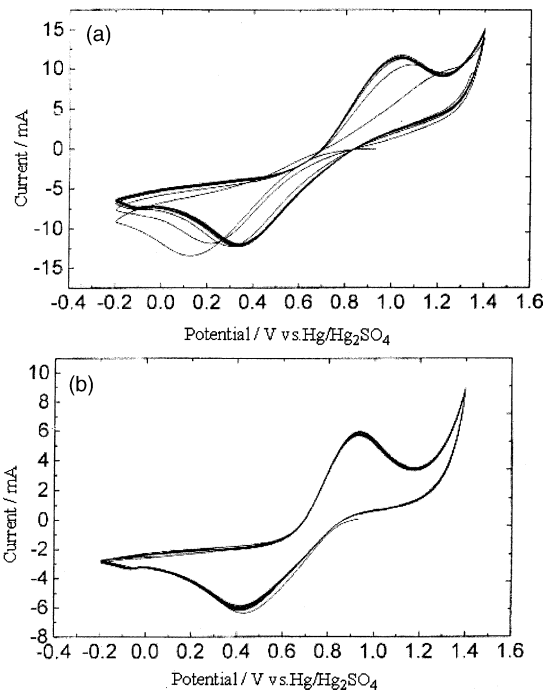


Fig. 3. Plot of cyclic voltammogram in  $0.3 \text{ mol dm}^{-3} \text{ Ce(SO}_4)_2 + 1.25 \text{ mol dm}^{-3} \text{ H}_2\text{SO}_4$  solution; sweep rate: (a)  $0.25 \text{ V s}^{-1}$  and (b)  $0.05 \text{ V s}^{-1}$  (between  $-0.2$  and 1.4 V).

This can only be attributed to the inhibition by platinum oxide to the oxidation of  $\text{Ce}^{3+}$ , which makes the anodic reaction move toward more positive values until it enters the oxygen-evolution area. While the sweep rate was low, the anodic peak current of  $\text{Ce}^{3+}$  could be observed and its peak potential was higher than in the sweep width  $-0.2$  to  $1.4$  V under the same sweep rate condition, the peak current decreased slightly. One possible reason was that the conductivity of platinum oxide formed at the surface of platinum was poor, which would add the resistance of the transfer of electrons. Another reason perhaps was that the platinum oxide occupied some active position on the surface of platinum; this would reduce the effective reaction sites at the same time as increasing the apparent surface area. Of course, it was also a possibility that the existence of platinum oxide changed the interfacial double layer structure between the solution and metal, causing a change of inner potential, which changed the electric field across the interface, and directly affected the transfer rate of electrons.

Kuhn and Randle [19] have reported that the type I platinum oxide existed in the form of  $\text{PtO}_2$ , and was a good electronic conductor; its conductivity was the same as platinum metal, but specific conductance of chemically prepared  $\text{PtO}_2$  powder was  $10^{-6} \Omega^{-1} \text{cm}^{-1}$  and behaved like semiconductors. However, the specific conductance of type I platinum oxide was much less  $[(1-2) \times 10^{-3} \Omega^{-1} \text{cm}^{-1}]$ . As a result, type I platinum oxide does not inhibit the charge-transfer process but type II platinum oxide may do so. In this paper pretreatment only produces type I platinum oxide, without type II platinum oxide (a type of platinum oxide which can only be produced by oxidize for more than 15 min at 1.7 V). Therefore, the inhibition of platinum oxide to the oxidation of  $\text{Ce}^{3+}$  was not due to the existence of type II platinum oxide. It was possible that the  $\text{Ce}^{3+}$  absorbed on the surface of platinum through the oxygen bridge and occupied the active position of surface, inhibiting the transfer of  $\text{Ce}^{3+}$  from the bulk solution, as a result making the anodic overpotential increase.

The reduction of  $\text{Ce}^{4+}$ , while the surface of platinum was covered with type I platinum oxide, is apparent in Fig. 2. The peak current was almost constant while the peak potential moved toward the cathodic direction, which demonstrated that although the charge-transfer was inhibited somehow (peak potential moved toward the cathodic direction), it could still reach the diffusion-controlling limiting current. It was generally accepted that  $\text{Ce}^{4+}$  would not absorb on the surface of the electrode, so the increase of cathodic overpotential was possible because of the inhibition by platinum oxide to the charge transfer.

### 3.2. Effect of initial $\text{Ce}^{4+}$ concentration on the $\text{Ce}^{4+}/\text{Ce}^{3+}$ couple

Fig. 4 shows the relation of cathodic peak current with the concentration of  $\text{Ce}^{4+}$  in  $1.25 \text{ mol dm}^{-3} \text{ H}_2\text{SO}_4$  solution. While the sweep rate is  $\leq 0.05 \text{ V s}^{-1}$ , a proportional

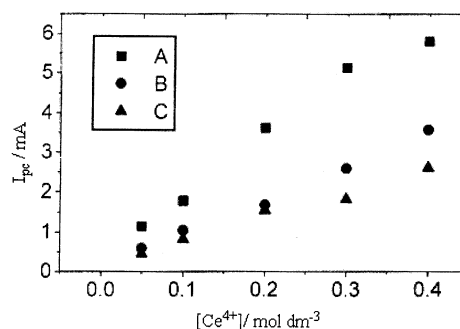


Fig. 4. Plots of cathodic peak current vs.  $\text{Ce}^{4+}$  concentration obtained for a Pt electrode in  $1.25 \text{ mol dm}^{-3} \text{ H}_2\text{SO}_4$  solution with different scan rates: (A)  $0.05 \text{ V s}^{-1}$ , (B)  $0.01 \text{ V s}^{-1}$  and (C)  $0.005 \text{ V s}^{-1}$ , at  $25^\circ\text{C}$ .

relationship could be obtained, which proved that the reduction current was only dependent on the reduction reaction of  $\text{Ce}^{4+} + \text{e}^- \rightarrow \text{Ce}^{3+}$ . On the other hand, the oxygen-evolution current was almost invariant when the concentration of  $\text{Ce}^{4+}$  changed, which proved that the existence of  $\text{Ce}^{4+}$  had no effect on the evolution of oxygen.

### 3.3. The effect of different state of charge (SOC) on the $\text{Ce}^{4+}/\text{Ce}^{3+}$ couple

Results of reduction  $0.4 \text{ mol dm}^{-3} \text{ Ce}(\text{SO}_4)_2$  in  $1.25 \text{ mol dm}^{-3} \text{ H}_2\text{SO}_4$  solution to 75 and 50% SOC, respectively, were shown in Table 1. From the cathodic reaction rate constant ( $k_c$ ), it was easy to observe that while the total concentration of cerium ions kept constant, the value of  $k_c$  firstly decreased from 100 to 75% SOC, then increased from 75 to 50% SOC, which showed that the polarizing resistance of 75% SOC electrolyte was much larger, while that of 50 and 100% SOC was relatively smaller. According to conventional hypothesis, with the increase of  $\text{Ce}^{3+}$  concentration and the decrease in the concentration of  $\text{Ce}^{4+}$ , the normal potential  $E^0$  should decrease, but here it was controversial. The value of  $E^0$  under 75% SOC increased to 0.76 V, almost the same as that of  $0.3 \text{ mol dm}^{-3} \text{ Ce}(\text{SO}_4)_2$  in  $0.5 \text{ mol dm}^{-3} \text{ H}_2\text{SO}_4$  solution, and the value of  $\alpha = 0.153$  was similar to that in the solution mentioned above ( $\alpha = 0.157$ ).

It seems that the electroactive substances may exist in different forms in  $0.5$  and  $1.25 \text{ mol dm}^{-3} \text{ H}_2\text{SO}_4$  solutions. The kinetic parameters of 75% SOC ( $0.4 \text{ mol dm}^{-3} \text{ Ce}(\text{SO}_4)_2$  in  $1.25 \text{ mol dm}^{-3} \text{ H}_2\text{SO}_4$  solution) were similar to those in  $0.5 \text{ mol dm}^{-3} \text{ H}_2\text{SO}_4$  solution with the same concentration

Table 1  
The kinetic parameters of  $0.4 \text{ mol dm}^{-3} \text{ Ce}(\text{SO}_4)_2$  in  $1.25 \text{ mol cm}^{-3} \text{ H}_2\text{SO}_4$  solution under various SOC

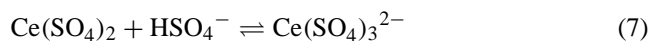
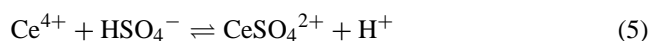
SOC (%)	$E^0$ (V)	$\alpha$	$\beta$	$k_c \times 10^4$ ( $\text{cm s}^{-1}$ )	$k_a \times 10^4$ ( $\text{cm s}^{-1}$ )
100	0.68	0.132		4.1	
75	0.76	0.153	0.230	2.18	3.13
50	0.74	0.155	0.197	2.99	2.93

of  $\text{Ce}^{4+}$ , therefore it was reasonable to believe that the electroactive substances of 75% SOC in  $1.25 \text{ mol dm}^{-3} \text{ H}_2\text{SO}_4$  solution were different from those in 100% SOC but just the same as the electroactive substances in  $0.5 \text{ mol dm}^{-3} \text{ H}_2\text{SO}_4$  solution. As a result, it was reasonable to think that the electroactive substances changed from 100 to 75% SOC were not simply due to the difference of  $\text{Ce}^{4+}$  concentration. Because when the concentration of  $\text{Ce}^{4+}$  decreased from 0.4 to 0.3,  $0.2 \text{ mol dm}^{-3}$  in  $1.25 \text{ mol dm}^{-3} \text{ H}_2\text{SO}_4$  solution,  $E^{0'}$  was 0.68, 0.682, 0.634 V, respectively, i.e. almost invariable, also  $k_c$  was similar, too:  $4.1 \times 10^{-4}$ ,  $4.03 \times 10^{-4}$  and  $3.6 \times 10^{-4} \text{ cm s}^{-1}$ , respectively. These results proved that the reactant in the reduction of  $\text{Ce}^{4+}$  in different concentration of  $\text{H}_2\text{SO}_4$  solution was the same. Therefore, the variation of  $E^{0'}$  and  $k_c$  at different SOC can only be attributed to the variation of  $\text{Ce}^{3+}$ . When  $\text{Ce}^{3+}$  absorbed on the surface of the oxide, it would make the oxidation of  $\text{Ce}^{3+}$  more difficult, and even lead to the anodic peak potential shifting positively more than 0.1 V when changing from 100 to 75% SOC with the same sweep rate.

### 3.4. The effect of different $\text{H}_2\text{SO}_4$ solution concentration on the $\text{Ce}^{4+}/\text{Ce}^{3+}$ couple

Because the  $\text{Ce}^{4+}$  undergoes hydrolysis when the concentration of  $\text{H}_2\text{SO}_4$  solutions is below  $0.5 \text{ mol dm}^{-3}$ , the concentration of  $\text{H}_2\text{SO}_4$  solution used here was above  $0.5 \text{ mol dm}^{-3}$ . Additionally, the purpose of this paper was to investigate the  $\text{Ce}^{4+}/\text{Ce}^{3+}$  couple used in a redox flow cell, and to improve the specific energy of electroactive substances in a unit volume, the concentration of  $\text{Ce}(\text{SO}_4)_2$  was as large as possible. But it was still an accepted fact that the solubility of  $\text{Ce}(\text{SO}_4)_2$  decreases with the increase of  $\text{H}_2\text{SO}_4$  concentration. Therefore, the maximum concentration of  $\text{H}_2\text{SO}_4$  used here was  $2 \text{ mol dm}^{-3}$ .

Figs. 1, 3 and 5 showed the cyclic voltammogram behavior of  $\text{Ce}(\text{SO}_4)_2$  in 2, 1.25 and  $0.5 \text{ mol dm}^{-3} \text{ H}_2\text{SO}_4$  solution. From the values of normal potential  $E^{0'}$  obtained from the cathodic and anodic peak potential, the distinct differences in 0.5, 1.25 and  $2 \text{ mol dm}^{-3} \text{ H}_2\text{SO}_4$  solutions are apparent. This demonstrated that in 1.25 and  $2 \text{ mol dm}^{-3} \text{ H}_2\text{SO}_4$  solutions  $\text{Ce}^{4+}$  existed in the same form of complex, but they were different from the complex ions in  $0.5 \text{ mol dm}^{-3} \text{ H}_2\text{SO}_4$  solution, and the complex in the former solution was more stable than that in the latter solution, the free  $\text{Ce}^{4+}$  was also low in the former solution so its normal potential was higher than that in the latter. In  $\text{H}_2\text{SO}_4$  solution, the  $\text{Ce}^{4+}$  could form the following complexes with  $\text{SO}_4^{2-}$ :



where the equilibrium constants are 3500, 200 and 20 [20] for reactions (5)–(7), respectively. While the concentration

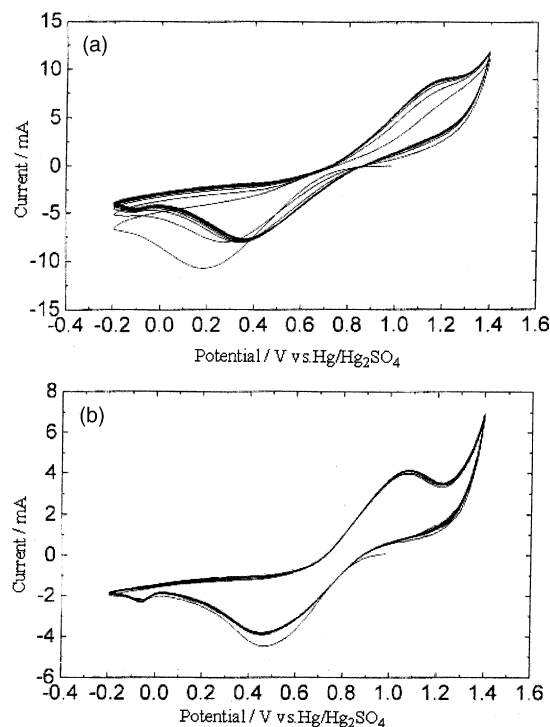


Fig. 5. Plot of cyclic voltammogram in  $0.3 \text{ mol dm}^{-3} \text{ Ce}(\text{SO}_4)_2 + 0.5 \text{ mol dm}^{-3} \text{ H}_2\text{SO}_4$  solution; sweep rate: (a)  $0.25 \text{ V s}^{-1}$  and (b)  $0.05 \text{ V s}^{-1}$ .

of  $\text{H}_2\text{SO}_4$  was  $0.5 \text{ mol dm}^{-3}$ ,  $[\text{Ce}^{4+}]/[\text{Ce}^{3+}] = 3/11$ , the parts of  $\text{Ce}(\text{SO}_4)_3^{2-}$  of the complexes were lower, and accordingly the free  $\text{Ce}^{4+}$  would be higher. But in 1.25 and  $2 \text{ mol dm}^{-3} \text{ H}_2\text{SO}_4$  solutions the ratio of  $[\text{Ce}^{4+}]/[\text{Ce}^{3+}] < 1/6$ , the three kinds of complexes could all exist in solution but the free  $\text{Ce}^{4+}$  may be correspondingly less.

From Table 2, it is clear that the reversibility of the  $\text{Ce}^{4+}/\text{Ce}^{3+}$  couple improved with increase of  $\text{H}_2\text{SO}_4$  concentration. As the  $\Delta E_p$  decreased with the increase of  $\text{H}_2\text{SO}_4$  concentration, the above two points showed that the  $\text{Ce}^{4+}/\text{Ce}^{3+}$  couple was not simply an one-electron transfer reaction:



but the reactant and product were concerned with  $\text{SO}_4^{2-}$  and  $\text{H}^+$ , Randle [11] reported that the possible reactions may be

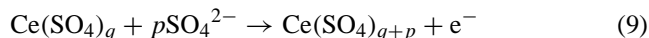


Table 2  
Effect of  $\text{H}_2\text{SO}_4$  concentration on  $\Delta E_p$  values of  $\text{Ce}^{4+}/\text{Ce}^{3+}$  couple at various sweep rates

$\text{H}_2\text{SO}_4$ ( $\text{mol dm}^{-3}$ )	Sweep rate ( $\text{V s}^{-1}$ )				
	0.25	0.1	0.05	0.01	0.005
2	0.664	0.54	0.462	0.32	0.262
1.25	0.706	0.594	0.522	0.374	0.316
0.5	0.849	0.697	0.622	0.382	0.34

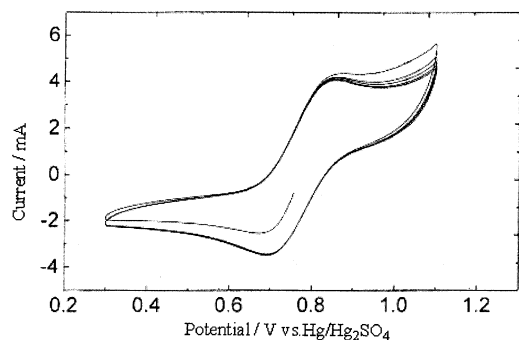
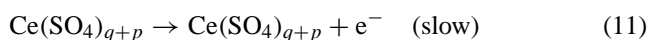
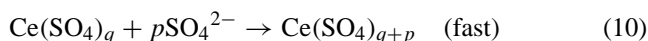


Fig. 6. Plot of cyclic voltammogram at Gr electrode in  $1.25 \text{ mol dm}^{-3}$   $\text{H}_2\text{SO}_4$  solution,  $[\text{Ce}^{4+}] = 0.3 \text{ mol dm}^{-3}$ ,  $[\text{Ce}^{3+}] = 0.1 \text{ mol dm}^{-3}$  (sweep rate is  $0.005 \text{ V s}^{-1}$ ).

or the kinetically indistinguishable mechanism:



The participating sulfate species may be  $\text{HSO}_4^-$  and not  $\text{SO}_4^{2-}$ .

### 3.5. The effect of different inert working electrodes on the $\text{Ce}^{4+}/\text{Ce}^{3+}$ couple

Figs. 3, 6 and 7 were the cyclic voltammogram results of the  $\text{Ce}^{4+}/\text{Ce}^{3+}$  couple at Pt, GC and Gr electrodes. Judged by the difference of anodic and cathodic peak potentials, the reversibility of the  $\text{Ce}^{4+}/\text{Ce}^{3+}$  couple at the Gr electrode was the best, then the GC electrode, and the Pt electrode was the poorest. It was clear that, at the surfaces of GC and Gr electrodes, while the sweep rate  $< 0.05 \text{ V s}^{-1}$ ,  $E_{\text{pc}}$ , little varied, when the sweep rate  $< 0.005 \text{ V s}^{-1}$ , the values of  $E_{\text{pa}}$  varied little, too. This proved that there was no absorption on the surface of GC, Gr electrodes, and the non-Faraday charge was slight. The overcharge was caused mostly by heterogeneous charge transfer. Because of the similarity of  $\Delta E_p$  between cathodic and anodic peak potential under different sweep rates, the values of  $\alpha$  and  $k_c$  could not be obtained

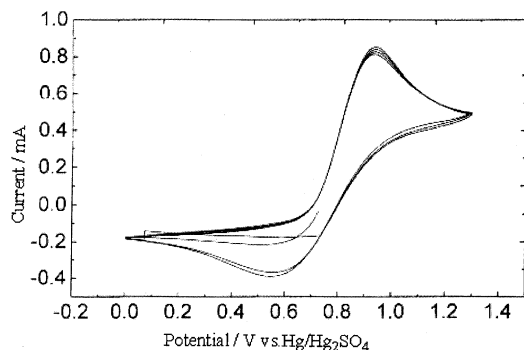


Fig. 7. Plot of cyclic voltammogram at GC electrode in  $0.5 \text{ mol dm}^{-3}$   $\text{H}_2\text{SO}_4$  solution,  $[\text{Ce}^{4+}] = 0.2 \text{ mol dm}^{-3}$ ,  $[\text{Ce}^{3+}] = 0.1 \text{ mol dm}^{-3}$  (sweep rate is  $0.005 \text{ V s}^{-1}$ ).

by Eq. (3). Within the scanning width of cyclic voltammogram ( $< 1.3 \text{ V}$ ), it was impossible to produce oxide on the surface of GC and Gr electrodes, so there was no inhibition to the oxidation of  $\text{Ce}^{3+}$ . But in the rotating ring disk electrode experiment [24], while the potential was above  $1.5 \text{ V}$ , a layer of oxidation film at the surface of GC electrode was produced.

## 4. Conclusions

Some conclusions can be surely drawn as follows. The type I platinum oxide with a specific conductance of  $10^{-6} \Omega^{-1} \text{ cm}^{-1}$  fully covered the surface of the electrode and inhibited the redox reaction to some extent. The forms of electroactive substances that existed in the solution varied a bit with different SOC of the  $\text{Ce}^{4+}/\text{Ce}^{3+}$  system. In addition, the  $\text{H}_2\text{SO}_4$  concentration had an apparent effect on the reversibility of  $\text{Ce}^{4+}/\text{Ce}^{3+}$  system, which could be clearly seen here with the increase of  $\text{H}_2\text{SO}_4$  concentration from  $0.5$  to  $2 \text{ mol dm}^{-3}$ —the reversibility of the system visibly improved. Finally, because of no adsorption of  $\text{Ce}^{4+}$  or  $\text{Ce}^{3+}$  and formation of oxides on the surface of GC and Gr electrodes, these carbon electrodes were more suitable for the  $\text{Ce}^{4+}/\text{Ce}^{3+}$  system than a platinum electrode. In short, the cyclic voltammogram results have demonstrated the feasibility of replacing  $\text{V}^{5+}/\text{V}^{4+}$  with a very high concentration of  $\text{Ce}^{4+}/\text{Ce}^{3+}$  to produce a completely novel redox cell.

## Acknowledgements

This work is financially supported by the National Natural Science Foundation of China, grant number 29963002.

## References

- [1] X. Xia, H. Liu, Y. Liu, J. Electrochem. Soc. 149 (2002) A426.
- [2] B. Fang, S. Iwasa, Y. Wei, T. Arai, M. Kumagai, Electrochim. Acta 47 (2002) 3971.
- [3] P.S. Fedkiw, R.W. Watts, J. Electrochem. Soc. 131 (1984) 701.
- [4] C.C. Liu, R.T. Galasco, R.F. Savinell, J. Electrochem. Soc. 129 (1982) 2502.
- [5] J. Gu, G.Q. Li, Q. Xu, Chinese J. Power Sources 24 (2000) 116.
- [6] A.J. Fenton, N.H. Furman, Anal. Chem. 29 (1957) 221.
- [7] J.J. Lingane, C.H. Langford, F.C. Anson, Anal. Chim. Acta 16 (1957) 165.
- [8] R. Kotz, S. Stucki, B. Carcer, J. Appl. Electrochem. 21 (1991) 14.
- [9] A. Mills, D. Worsley, J. Chem. Soc., Faraday Trans. 87 (1991) 3275.
- [10] A. Mills, S. Giddings, Inorg. Chim. Acta 16 (1957) 165.
- [11] T.H. Randle, A.T. Kuhn, J. Chem. Soc., Faraday Trans. I 79 (1983) 1741.
- [12] S. Ferro, A.D. Battisti, Phys. Chem. Chem. Phys. 4 (2002) 1915.
- [13] Y. Meada, K. Sato, R. Ramaraj, Electrochim. Acta 44 (1999) 3441.
- [14] E. Bishop, P. Cofve, Analyst 106 (1981) 316.
- [15] A. Paulenova, S.E. Creager, J.D. Navratil, Y. Wei, J. Power Sources 109 (2002) 431.
- [16] T.H. Randle, A.T. Kuhn, Aust. J. Chem. 42 (1989) 229.

- [17] T.H. Randle, A.T. Kuhn, *Aust. J. Chem.* 42 (1989) 1527.
- [18] P. Klekens, L. Steen, H. Ponche, *Electrochim. Acta* 26 (1981) 841.
- [19] A. Kuhn, T.H. Randle, *J. Chem. Soc., Faraday Trans. I* 81 (1985) 403.
- [20] R.A. Bonewitz, G.M. Schmid, *J. Electrochem. Soc.* 117 (1970) 1367.
- [21] R. Zingales, *J. Chem. Soc., Dalton Trans.* (1990) 229.
- [22] D. Pleecher, E.M. Valdes, *Electrochim. Acta* 33 (1988) 499.
- [23] A.H. Kunz, *J. Am. Chem. Soc.* 53 (1931) 98.
- [24] X. Xia, H. Liu, Y. Liu, *Acta Chim. Sin.* 59 (2001) 2063.
- [25] X. Xia, H. Liu, Y. Liu, *Acta Chim. Sin.* 60 (2002) 1630.
- [26] A.J. Bard, L.R. Faulkner, *Electrochemical Methods—Fundamental and Application*, Wiley, New York, 1980.
- [27] E. Sum, M. Skyllas-Kazacos, *J. Power Sources* 15 (1985) 179.